We can then substitute $\langle I \rangle$ for S in Eq. 139, to find

(146)
$$S = I - \mu \frac{dI}{d\tau}$$

(147)
$$\langle I \rangle = I - \mu \frac{dI}{d\tau}$$

(148)
$$\frac{1}{2} \int_{-1}^{1} I d\mu = I - \mu \frac{dI}{d\tau}$$

This is an integro-differential equation for gray atmospheres in radiative equilibrium. Though it looks odd, it is useful because an exact solution exists. After finding $\langle I \rangle = S$, we can use our formal solutoin to the radiative transfer equation to show that

(149) $$S = \frac{3F_0}{4\pi} [\tau + q(\tau)]$$

where F_0 is the input flux at the base of the atmosphere and $q(\tau)$ is the Hopf function, shown in Fig. 17. Let's examine an approximation to this function that provides a lot of insight into what's going on.

We'll start by examining the moments of the radiative transfer equation, where moment n is defined as

(150) $$\mu^{n+1} \frac{\partial I}{\partial \tau} d\Omega = \int \mu^n (I - S) d\Omega$$

We already did $n = 0$ back in Eq. 143, so let's consider $n = 1$. We'll need each

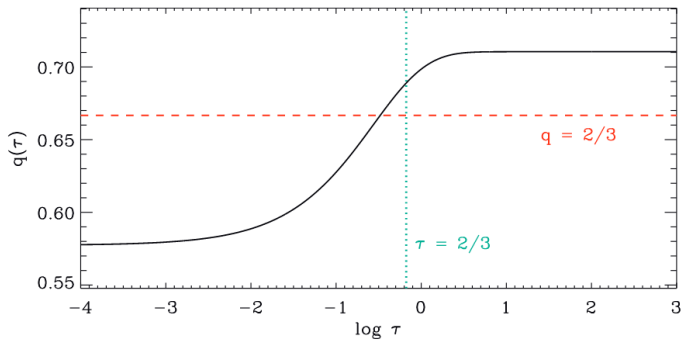

Figure 17: Hopf function $q(\tau)$, which has as its limits $q(0) = 1/\sqrt{3}$ and $q(\infty) = 0.7101....$

of the following terms, given in Eqs. 151–153:

$$\int \mu S d\Omega = 2\pi S \int_{-1}^{1} \mu d\mu \tag{151}$$

which equals zero, since S is isotropic.

$$\int \mu I d\Omega \equiv F \tag{152}$$

(the definition of flux), and finally

$$\int \mu^2 I d\Omega = \int I \cos^2\theta d\Omega \equiv c P_{\rm rad} \tag{153}$$

from Eq. 58.

The first moment then becomes

$$c\frac{dP}{d\tau} = F \tag{154}$$

which we have required to be constant. Thus, we find that

$$P_{\rm rad} = \frac{F}{c}(\tau + Q) \tag{155}$$

where here Q is a constant of integration; when certain assumptions are lifted, this becomes the Hopf function $q(\tau)$ of Fig. 17.

9.3 *The Eddington Approximation*

Eq. 155 is a potentially powerful result, because it tells us that in our gray, flux-conserving atmosphere the radiation pressure is just a linear function of the bolometric flux. This will become even more useful, since we are about to connect this back to S, and thence to I (a more useful observational diagnostic than P).

From the expression for the radiation pressure of a blackbody field (Eq. 58) we have that

$$P = \frac{4\pi}{3c}\int B_\nu d\nu \tag{156}$$

$$= \frac{4\pi}{3c} S \tag{157}$$

since we assume LTE, and thus our source function is the Planck function. *However*, remember that our atmosphere exhibits a temperature gradient, so our radiation field isn't actually a pure blackbody. We therefore make the key assumption — the **Eddington approximation** — that the temperature gradient is weak enough that the abov expression for P is valid (correcting this

assumption turns Q into $q(\tau)$).

Under these assumptions, we then combine Eq. 157 and 155 to find

(158)
$$S = \frac{3F}{4\pi}(\tau + Q)$$

(159)
$$= \frac{3F}{4\pi}\left(\tau + \frac{2}{3}\right)$$

Thus the stellar atmosphere's source function is just a linear function of optical depth – just as we had blithely assumed in Eq. 137 when introducing limb darkening. The value of $2/3$ comes from a straightforward but tedious derivation described in Sec. 2.4.2 of the Choudhuri textbook.

We can also use Eq. 159 to clarify our previous discussion of limb darkening. Since we now know the particular linear dependence of S on τ, we can dispense with the arbitrary constants in Eq. 138 to show that the emergent intensity is

(160) $$I(\tau = 0, \mu) = \frac{3F}{4\pi}\left(\mu + \frac{2}{3}\right)$$

which shows decent agreement with observational data. This type of expression is called a **linear limb-darkening "law"**. Because of our assumptions this doesn't perfectly fit observed stellar limb-darkening profiles, so there is a whole family of various relations that people use (some physically justified, some empirical).

Finally, given the exact functional form of S in Eq. 159, we can now compute the stellar atmosphere's **thermal structure** – how its temperature changes with optical depth, pressure, or altitude. This relation is derived by relating S to the Stefan-Boltzmann flux F from Eq. 60:

(161)
$$S = \int S_\nu d\nu$$

(162)
$$= \int B_\nu d\nu$$

(163)
$$= \frac{\sigma_{SB} T^4}{\pi}$$

(as for that factor of π, see Sec. 1.3 of the Rybicki & Lightman). We now have $S(T)$ as well as $S(\tau)$, so combining Eqs. 159, Eq. 163, and the Stefan-Boltzmann flux (Eq. 60) we obtain a relation that

(164) $$T^4(\tau) = \frac{3}{4} T_{\text{eff}}^4 \left(\tau + \frac{2}{3}\right)$$

This gives us the thermal profile through the star's atmosphere. As we move deeper into the star the vertical optical depth τ increases (Eq. 130) and the temperature rises as well (Eq. 164). Note too that the atmospheric temperature $T = T_{\rm eff}$ when $\tau = 2/3$. Earlier we have claimed that we see down to a depth of $\tau \approx 1$, so we have no refined that statement to say that we see into a stellar atmosphere down to the $\tau = 2/3$ surface.

9.4 *Frequency-Dependent Quantities*

We've achieved quite a bit, working only with frequency-integrated quantities: in particular, the temperature structure in Eq. 164 and the formal solution Eq. 135. However, although our earlier treatment of excitation and ionization of atomic lines (Sec. 8.5) qualitatively explains some of the trends in absorption lines seen in stellar spectra, we have so far only discussed line formation in the most qualitative terms.

We expect intensity to vary only slowly with frequency when temperatures are low. This because we expect the ratio $R(\nu)$ between intensities at two temperatures to scale as:

(165)
$$R(\nu) = \frac{I_\nu(T_B)}{I_\nu(T_A)}$$

(166)
$$\approx \frac{B_\nu(T_B)}{B_\nu(T_A)}$$

(167)
$$= \frac{e^{h\nu/kT_A} - 1}{e^{h\nu/kT_B} - 1}$$

This is consistent with the observed frequency dependence of limb darkening, which is seen to be much weaker at longer (infrared) wavelengths and stronger at shorter (e.g., blue-optical) wavelengths.

Let's now consider a more empirical way to make progress, based on the fact that we can observe the intensity emerging from the top of the atmosphere, $I_\nu(\tau_\nu = 0, \mu)$, across a wide range of frequencies. Expanding on our earlier, linear model of S_ν (Eq. 137), a fully valid expression for the source function is always

(168) $$S_\nu = \sum_{n=0}^{\infty} a_{\nu,n} \tau_\nu^n$$

Putting this into our formal solution, Eq. 135, and invoking the defintion of the gamma function gives

(169) $$I_\nu(0, \mu) = \sum_{n=0}^{\infty} a_{\nu,n}(n!)\mu^n$$

So long as we are in LTE, then we also have $S_\nu(\tau_\nu) = B_\nu[T(\tau_\nu)]$. This lets us

map out $T(\tau_\nu)$, which we can do for multiple frequencies – as shown in Fig. 18. Each T corresponds to a particular physical depth in the stellar atmosphere, so we have successfully identified a mapping between optical depth, frequency, and temperature.

Since for any ν we typically observe only down to a constant $\tau_\nu \approx 2/3$, we can rank the absorption coefficients α_{ν_i} for each of the ν_i sketched in Fig. 18. For any given τ_ν, $T(\tau_\nu)$ is greatest for ν_1 and least for ν_3. Thus we are seeing deepest into the star at ν_1 and α_{ν_1} must be relatively small, while on the other hand we see only to a shallow depth (where T is lower) at ν_3 and so α_{ν_3} must be relatively large.

9.5 *Opacities*

What affects a photon as it propagates out of a stellar atmosphere? So far we haven't talked much about the explict frequency dependence of α_ν, but this is essential in order to interpret observations.

From the definition of α_ν in Eq. 69, one sees that

(170) $n\sigma_\nu = \rho\kappa_\nu$

A lot of work in radiative transfer is about calculating the opacity κ_ν given ρ, T, and composition. In practice most desired opacities are tabulated and one uses a simple look-up table for ease of calculation. Nonetheless we can still consider some of the basic cases. These include:

1. Thomson (electron) scattering
2. Bound-bound reactions
3. Bound-free: phototionization & recombination
4. Free-free: Bremsstrahlung

Thomson scattering

The simplest effect is **Thomson scattering**, also known as electron scattering. In this interaction a photon hits a charged particle, shakes it up a bit (thus

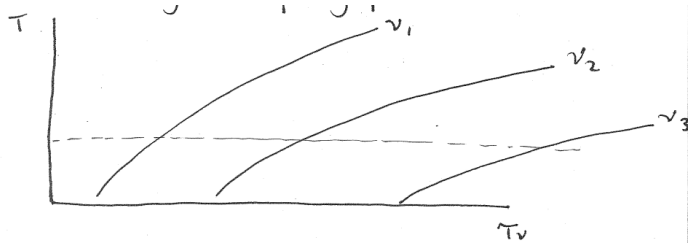

Figure 18: Notional atmospheric structure, $T(\tau_\nu)$, with different frequencies ν_i.

taking energy out of the radiation field), and is then re-radiated away. The basic (frequency-independent) cross-section is derived in many text books (e.g. Rybicki & Lightman, Sec. 3.4), which shows that in cgs units,

$$\sigma_T = \frac{8\pi}{3}\left(\frac{e^2}{m_e c^2}\right)^2 \tag{171}$$

or approximately $2/3 \times 10^{-24}$ cm^2.

Notice that $\sigma_T \propto m^{-2}$, so the lightest charge-carriers are the most important – this means electrons. Eq. 171 suggests that in a notional medium composed solely of electrons, we would have

$$\kappa_\nu = \frac{n_e \sigma_T}{\rho_e} = \frac{\sigma_T}{m_e} \tag{172}$$

In any real astrophysical situation our medium will contain a wide range of particles, not just electrons. So in actuality we have

$$\kappa_\nu = \frac{n_e \sigma_T}{\rho_{\rm tot}} \equiv \frac{1}{\mu_e}\frac{\sigma_T}{m_p} \tag{173}$$

where we have now defined the **mean molecular weight of the electron** to be

$$\mu_e = \frac{\rho_{tot}}{n_e m_p} \tag{174}$$

The quantity μ_e represents the mean mass of the plasma per electron, in units of m_p (note that this is a bit different from the mean molecular weight for ions, which is important in stellar interior calculations). But in a fully ionized H-only environment, $n_e = N$ cm^{-3} while $\rho = Nm_p$ cm^{-3} — so $\mu_e = 1$. Meanwhile in a fully ionized, 100% He plasma, $n_e = 2N$ cm^{-3} while $\rho = 4N$ cm^{-3} — so in this case, $\mu_e = 2$.

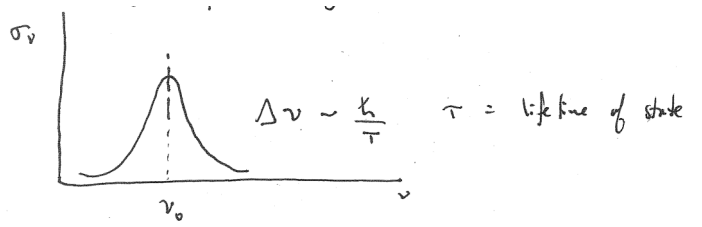

Figure 19: Schematic of σ_ν for bound-bound reactions, showing a line centered at ν_0 and with intrinsic width $\Delta\nu \sim \hbar/\tau$.

Bound-bound transitions

As the name implies, these involve changes between energy levels that still leave all particles bound. Most stellar opacity sources are of this type, which give rise to lines such as those depicted schematically in Fig. 19. In all cases the *intrinsic* line width $\Delta\nu \sim \hbar/\tau$ is given by the Heisenberg uncertainty principle and by τ, the typical lifetime of the state.Depending on the system being studied. But τ can change considerably depending on the system under analysis.

The general expression for the line's cross-section will be that

$$\sigma_\nu = \frac{\pi e^2}{m_e c} f \Phi(\nu - \nu_0) \tag{175}$$

where f is the transition's dimensionaless oscillator strength (determined by the atomic physics) and $\Phi(\nu - \nu_0)$ is the line profile shape as sketched in Fig. 19. Note that Eq. 175 will also sometimes be written not in terms of f but rather as

$$\sigma_\nu = \frac{B_{LU} h\nu}{4\pi} \Phi(\nu - \nu_0) \tag{176}$$

where B_{LU} is the "Einstein B" coefficient for the transition from the lower to the upper state.

Regardless, the lifetime of the state may be intrinsic (and long-lived) if the particles involved are isolated and non-interacting, and undergo only **spontaneous emission**. This gives rise to the narrowest lines, which are said to be **naturally broadened.**

When conditions are denser and the particle interaction timescale $\lesssim \tau$, then collisions perturb the energy levels and so slightly higher- or lower-energy photons can couple to the particles involved. This leads to **pressure broadening** (or collisional broadening), which leads (as the name implies) to broader lines in higher-pressure environments.

Finally, particle velocities will impart a range of Doppler shifts to the observed line profile, causing various types of extrinsic broadening. In general these can all be lumped under the heading of **Doppler broadening**, in which the line width is set by the material's velocity,

$$\frac{\Delta\nu}{\nu_0} = \frac{v_r}{c} \tag{177}$$

This is an important effect for the accretion (or other) disks around black holes and around young stars, and also for the nearly-solid-body rotation of individual stars.

There's a lot more to say about bound-bound transitions than we have time for here. But whatever the specific situation, our approach will always be the following: use the Saha and Boltzmann equations to establish the populations in the available energy levels; then use atomic physics to determine the oscillator strength f and line profile $\Phi(\nu - \nu_0)$.

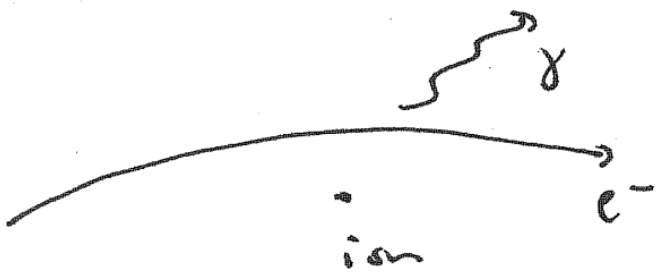

Figure 20: Bremsstrahlung (braking radiation) — an electron decelerates near an ion and emits a photon.

Bremsstrahlung

If you speak German, you might recognize that this translates as "braking radiation" — and Bremsstrahlung (or "free-free") is radiation caused by the deceleration of charged particles (typically electrons), as shown schematically in Fig. 20. Under time reversal, this phenomenon also represents absorption of a photon and acceleration of the electron. Typically this is modeled as occuring as the e^- is near (but not bound to) a charged but much more massive ion, which is assumed to be stationary during the interaction. Rybicki & Lightman devote a whole chapter to Bremsstrahlung, but we'll just settle for two useful rules of thumb:

(178) $\alpha_\nu^{ff} \approx 0.018 T^{-3/2} Z^2 n_e n_i \nu^{-2} \bar{g_{ff}}$

and

(179) $\epsilon_\nu^{ff} \approx (6.8 \times 10^{-38}) Z^2 n_e n_i T^{-1/2} e^{-h\nu/kT} \bar{g_{ff}}$

where Z is the ionic charge and $\bar{g_{ff}}$ is the **Gaunt factor**, typically of order unity.

Bound-free

In this case, electrons transition between a bound (possibly excited) state and the free (i.e., ionized) state. If the initial state is bound, then an incoming photon comes in and (possibly) ejects an electron. Thus the e^- begins within a series of discretized, quantum, atomic energy levels and ends unbound, with a continuum of energy levels available to it. A full derivation shows that for a given bound transition we find $\sigma_\nu \propto \nu^{-3}$. But as ν decreases toward the ionization threshold ν_i (e.g., 13.6 ev$/h$ for H in the ground state), then σ_ν will sharply drop when the photon is no longer able to ionize. But assuming there is some excited hydrogen (e.g., ν_2=13.6$/4h$ for H in the $n = 2$ state), then there will be a second one-sided peak located at ν_2, and so on as shown in Fig. 21.

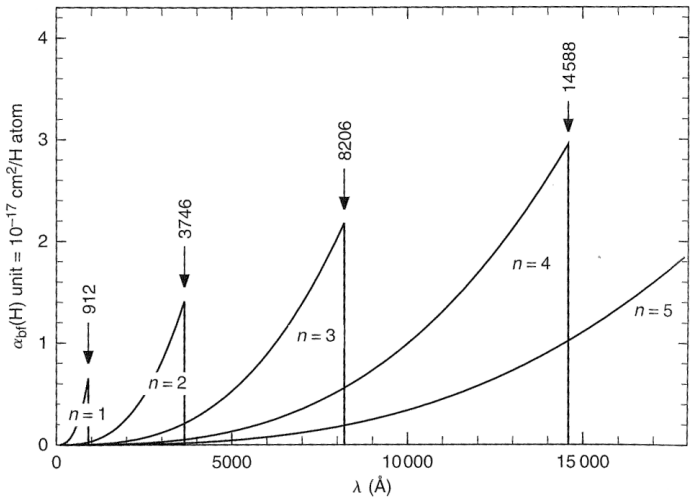

Figure 21: Extinction coefficient α_ν for bound-free transitions of the H atom (from Gray's *Stellar Photospheres*, Fig. 8.2). The characteristic scaling with $\nu^{-3} \propto \lambda^3$ is clearly apparent.

H-minus opacity

For years after astronomers first turned their spectrographs toward the Sun, it was unclear which processes explained the observed Solar opacity. It was apparent that the opacity was fairly large, despite the fact that H and He are almost entirely neutral in the Solar photosphere and bound-bound transitions also weren't able to explain the data.

The solution turned out to be the **negative hydrogen ion**, H^-, which is stable because the normal H atom is highly polarized and can hold another e^-. The electron is bound only weakly, with a dissociation energy of just 0.75 eV (no stable, excited states exist). Thus all photons with $\lambda \lesssim 1.7\mu$m can potentially break this ion and, being absorbed, contribute to an overall continuum opacity that is strongest from 0.4–1.4μm. The magnitude of the total H^- opacity depends sensitively on the ion's abundance: it drops off steeply in stars much hotter than the Sun (when most H^- is ionized) and in the very coolest stars (when no free e^- are available to form the ion). In addition to being a key opacity source in many stars, H^- has only recently been recognized as a key opacity source in the atmospheres of the hottest extrasolar planets (see e.g. Lothringer et al., 2018).